



**HAL**  
open science

# Properties of AKR-Like Emissions Recorded by the Low Altitude Satellite DEMETER During 6.5 Years

M. Parrot, F. Němec, O. Santolík

## ► To cite this version:

M. Parrot, F. Němec, O. Santolík. Properties of AKR-Like Emissions Recorded by the Low Altitude Satellite DEMETER During 6.5 Years. *Journal of Geophysical Research Space Physics*, 2022, 127 (6), 10.1029/2022JA030495 . insu-03697281

**HAL Id: insu-03697281**

**<https://insu.hal.science/insu-03697281>**

Submitted on 16 Jun 2022

**HAL** is a multi-disciplinary open access archive for the deposit and dissemination of scientific research documents, whether they are published or not. The documents may come from teaching and research institutions in France or abroad, or from public or private research centers.

L'archive ouverte pluridisciplinaire **HAL**, est destinée au dépôt et à la diffusion de documents scientifiques de niveau recherche, publiés ou non, émanant des établissements d'enseignement et de recherche français ou étrangers, des laboratoires publics ou privés.

Copyright

# JGR Space Physics

## RESEARCH ARTICLE

10.1029/2022JA030495

## Properties of AKR-Like Emissions Recorded by the Low Altitude Satellite DEMETER During 6.5 Years

M. Parrot<sup>1,2</sup> , F. Němec<sup>3</sup>, and O. Santolík<sup>3,4</sup> 

<sup>1</sup>LPC2E/CNRS, Orléans, France, <sup>2</sup>University of Orléans, Orléans, France, <sup>3</sup>Faculty of Mathematics and Physics, Charles University, Prague, Czech Republic, <sup>4</sup>Department of Space Physics, Institute of Atmospheric Physics of the Czech Academy of Sciences, Prague, Czech Republic

### Key Points:

- Numerous auroral kilometric radiation-like events have been recorded by the low-altitude satellite DEMETER during moderate and high magnetic activity
- There are more events in the Northern than in the Southern hemisphere but this difference decreases when the auroral activity increases
- The number of events decreases in winter in each hemisphere

### Correspondence to:

M. Parrot,  
[mparrot@cns-orleans.fr](mailto:mparrot@cns-orleans.fr)

### Citation:

Parrot, M., Němec, F., & Santolík, O. (2022). Properties of AKR-like emissions recorded by the low altitude satellite DEMETER during 6.5 years. *Journal of Geophysical Research: Space Physics*, 127, e2022JA030495. <https://doi.org/10.1029/2022JA030495>

Received 24 MAR 2022  
Accepted 31 MAY 2022

### Author Contributions:

**Conceptualization:** M. Parrot  
**Data curation:** M. Parrot  
**Investigation:** M. Parrot, F. Němec, O. Santolík  
**Methodology:** M. Parrot, F. Němec, O. Santolík  
**Validation:** F. Němec, O. Santolík  
**Writing – original draft:** M. Parrot  
**Writing – review & editing:** F. Němec, O. Santolík

**Abstract** Normally, auroral kilometric radiation (AKR) which is emitted in the auroral zones escapes from the Earth. But since a few decades very similar radiations are observed by ground-based receivers and by satellites at altitudes below the AKR generation area. They are called leaked AKR or AKR-like emissions because it is expected that there are linked to AKR. This paper deals with observations of such AKR-like emissions observed in the auroral zones (in the North and in the South) by the low-altitude satellite DEMETER. In total, 2,526 events have been recorded during 6.5 years. These events are not very rare as they occur at least 2% of the time. Although this data set has a severe flaw due to a latitudinal constraint, it was possible to draw interesting properties of these emissions. In fact they are very similar to usual AKR observed at much higher altitudes during auroral activities (the same frequency range, magnetic local time (MLT) sector, and invariant latitude). The main difference concerns a strong asymmetry between the Northern and the Southern hemispheres: (a) the number of AKR-like emissions in the Northern hemisphere is 32% larger than in the Southern hemisphere but this percentage decreases when the auroral activity increases, and (b) there is an important seasonal effect because the number of events decreases during the winter season both in the North and in the South.

**Plain Language Summary** Auroral kilometric radiation (AKR) is the strongest terrestrial radio emission generated between 30 and 800 kHz along the auroral field lines and associated with a discrete auroral arc. This emission is generated by superthermal electrons (several keV) which are injected from the magnetotail when the solar activity increases. Typical location of the source is  $\sim 22$  hr of magnetic local time (MLT),  $\sim 70^\circ$  of invariant latitude, and  $(2-10)10^3$  km of altitude. AKR propagates from the Earth and should not be able to reach low altitudes because of the ionospheric frequency cutoff. But a few decades ago, AKR-like emissions have been recorded by low orbiting satellites and even by ground-based receivers. It was explained by a mode conversion of the wave propagating in inhomogeneous plasma. Up to now, only studies of some AKR-like events have been reported, and this paper presents the statistical properties of such emissions recorded by the low altitude satellite DEMETER during 6.5 years. AKR-like emissions display similar characteristics of AKR in terms of frequency, MLT, and invariant latitude. It is shown that more events are observed in the North than in the South, and that there is a seasonal effect (the number of events decreases in winter hemispheres).

## 1. Introduction

Auroral kilometric radiation (AKR) was first observed by ELECTRON 2 satellite in 1965 (Benediktov et al., 1965, 1966), and a comprehensive study of these emissions has been done by Gurnett (1974). They are generated at frequencies between 50 and 500 kHz during substorms on the field lines of discrete auroras above the auroral oval mainly during nighttime (22 hr in magnetic local time [MLT]). On average they are located at  $70^\circ$  of invariant latitude, and  $1.5-3 R_E$  of altitude (Gurnett, 1974; Kurth et al., 1975). The generation mechanism of the AKR is related to the electron Cyclotron Maser Instability (CMI) at frequencies close to the electron cyclotron frequency (Alexander & Kaiser, 1976; Wu & Lee, 1979; see also the review by Louarn [2006]).

AKR is escaping from the Earth and their frequencies being well below the cutoff frequencies of the ionosphere (on average 10 MHz during daytime and 3 MHz during night time), this emission should not be observable at low altitudes. However, low-altitude satellites have observed Medium Frequency (MF, 300 kHz–3 MHz) waves in the same frequency range (Benson & Wong, 1987; Oya et al., 1985), and similar waves have been even registered by ground-based receivers (Benson et al., 1988; LaBelle & Anderson, 2011; LaBelle et al., 2015, 2022). Using

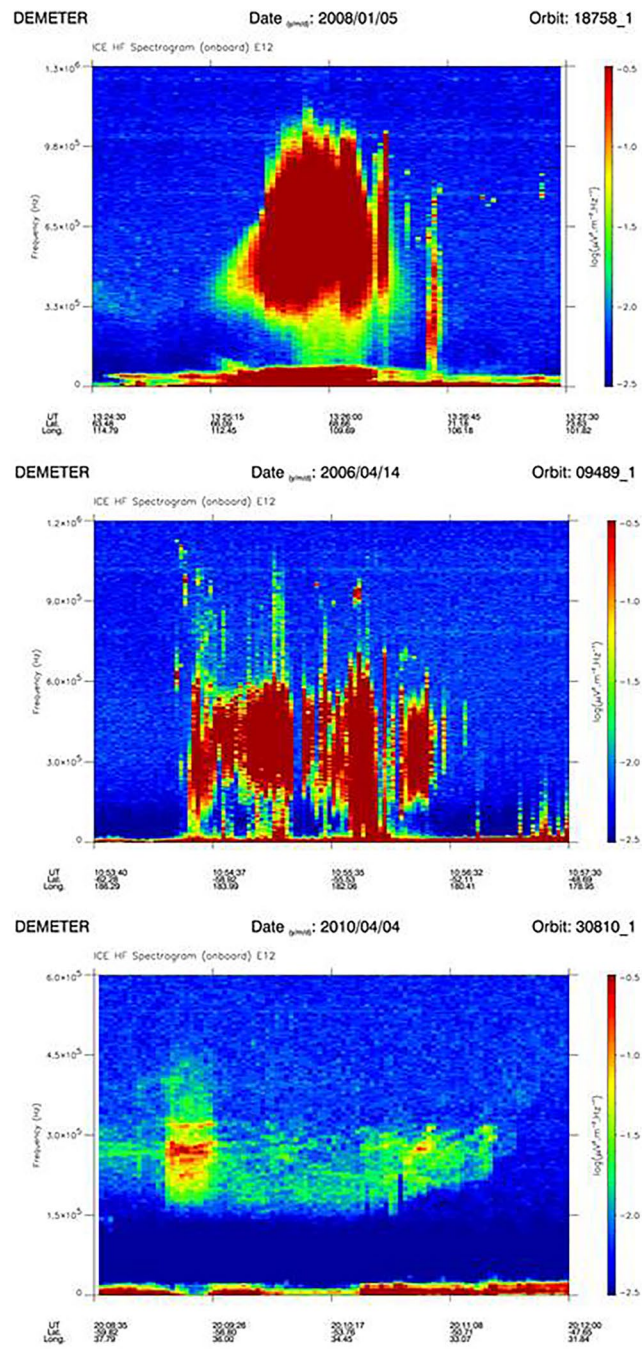


**Figure 1.** Examples of auroral kilometric radiation-like emissions observed by DEMETER. (top panel) emissions recorded on 5 January 2008 between 13:24:30 and 13:27:30 UT in the frequency range 0–1.3 MHz; (middle panel) emissions recorded on 14 April 2006 between 10:53:40 and 10:57:30 UT in the frequency range 0–1.2 MHz; (bottom panel) emissions recorded on 4 April 2010 between 20:08:35 and 20:12:00 UT in the frequency range 0–600 kHz. The intensity of the emissions is color coded according to the scale on the right of each panel. The parameters at the bottom of each panel are the geographic latitude and longitude.

EXOS-C data, Oya et al. (1985) were the first to attribute these emissions to leakage of the AKR. They called them leaked AKR. LaBelle and Anderson (2011) have compared three examples of AKR-like emissions detected at a South Pole station in Antarctica, with data from the Geotail satellite. These AKR-like emissions detected at ground-level have the same frequency-time structure as simultaneous AKR emissions detected on Geotail far from the Earth. This was confirmed with many other events by LaBelle et al. (2015). They show that the occurrence

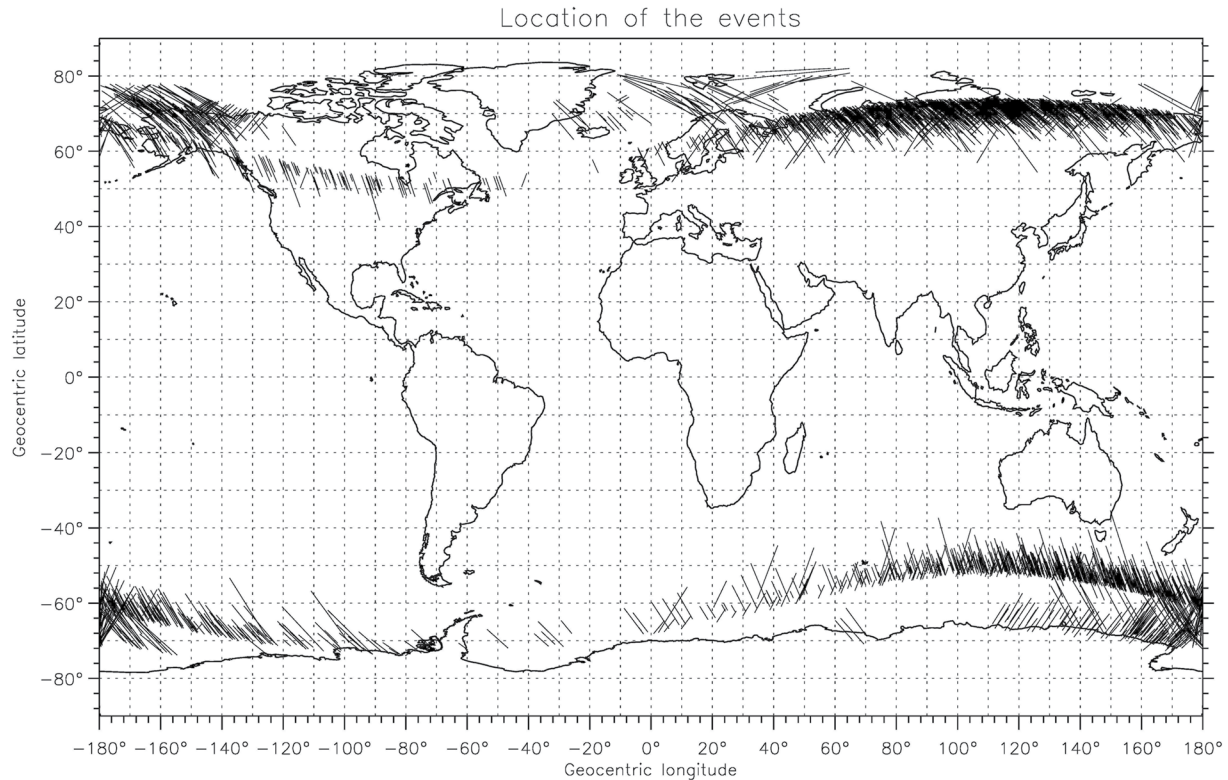


**Figure 2.** Locations of the 2,526 events. The length of each segment corresponds to the duration of the observed events.

rate peaks near 22:00 MLT similar to that of AKR. Later on, LaBelle et al. (2022) have compared data from their South Pole receivers with the Wide Band Data (WBD) of Cluster satellites during 35 time intervals in 2018–2020. In the two data sets, they have simultaneously observed similar types of AKR with fine structures.

Several processes have been proposed to explain these observations (Krasovskiy et al., 1983; LaBelle & Anderson, 2011; LaBelle et al., 2015; Oya et al., 1985; Treumann et al., 2018). It is expected that the penetration of AKR to low altitudes must be related to CMI which can excite Z-mode emissions in regions close to X-mode emissions (Mutel et al., 2011). In inhomogeneous plasma, Z-mode waves can be converted to whistler-mode waves which can propagate in ionospheric dense plasma and reach the ground level. These various modes of wave propagation are well illustrated in the dispersion diagrams (wave frequency vs. wave number) shown in Figure

1 of Carpenter et al. (2003). A complete review of the possible mechanisms to explain AKR-like emissions can be found in the recent study by LaBelle et al. (2022).

A preliminary study of AKR-like emissions recorded by the low altitude DEMETER satellite during the super magnetic storm of November 2004 has been done by Parrot and Berthelier (2012). This paper supplements this previous analysis and reports all observations of these emissions both in the northern and southern auroral regions during 6.5 years. Section 2 describes the data. Section 3 presents the observations and the statistical features. Section 4 is devoted to discussion and conclusions.

## 2. The DEMETER Data

DEMETER was a low-altitude satellite (660 km) in operation between 2004 and 2010 on a polar and circular orbit. It measured electromagnetic waves and plasma parameters all around the Earth. The orbit of DEMETER was nearly sun-synchronous. The Electric Field Instrument (ICE) measures the

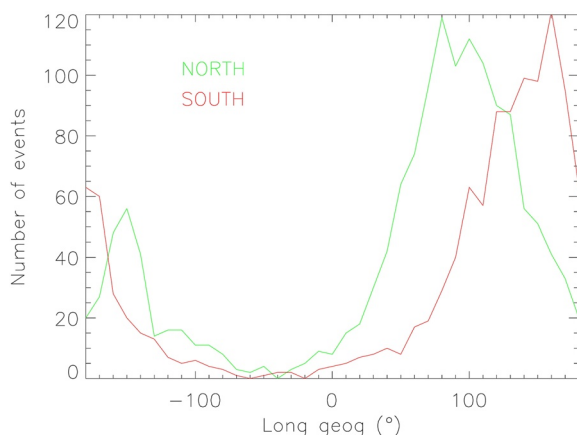


**Figure 3.** Number of events as a function of the geographic longitude in the Northern auroral zone (green) and in the Southern auroral zone (red).

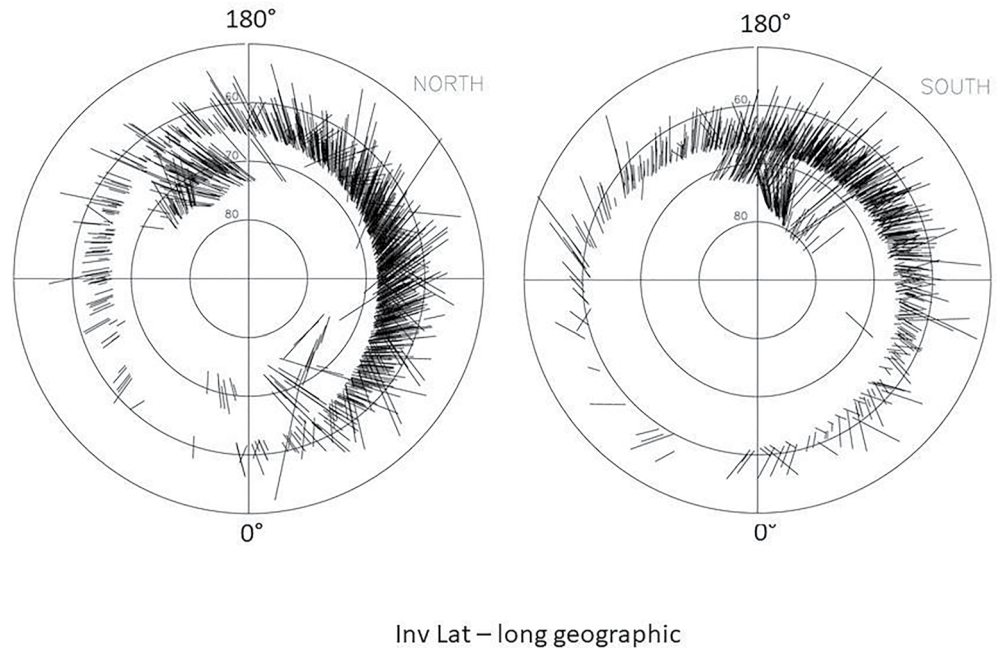


**Figure 4.** Same data as in Figure 2 but displayed in two polar plots as a function of the invariant latitude and the geographic longitude in the Northern (left) and Southern (right) hemisphere.

three electric components of plasma waves in the frequency range from DC to 3.25 MHz. A detailed description can be found in Berthelier et al. (2006). Data presented in this paper are onboard calculated to produce 2.048 s averaged MF power spectra of one electric component with a frequency resolution of 3.25 kHz. The MF spectrograms (0–3.25 MHz) of the quick-looks (summary plots of each experiment) have been visually checked to find intense emissions at high latitudes. The data handling has been organized in order to have a quick-look for each half-orbit. The descending half-orbit corresponds to daytime (10:00 LT) and the ascending half-orbit corresponds to nighttime (22:00 LT). During the lifetime of DEMETER there were 34,571 orbits which normally must give 69,142 quick-looks. But due to various reasons (satellite operations, occurrences of safe mode from time to time, Single-Event Upsets, and onboard memory full) only 57,761 quick-looks are available. This gives 115,522 opportunities to look at data over the auroral zone either in the North or in the South. An important constraint is that the record of the data has been stopped at very high latitudes because the auroral zone was not a key area for the main scientific objectives of the mission. However, during special campaigns, registrations have been occasionally done above HAARP (High Frequency Active Auroral Research Program) in Alaska, EISCAT (European

Incoherent Scatter radar) in Scandinavia and their magnetically conjugate regions. In total, 2,526 events (AKR-like emissions) have been detected in the MF plots of the quick-looks (1,437 in the North and 1,089 in the South). Due to the latitudinal limit most of them are cut at the beginning or at the end of a half-orbit. Nevertheless, 252 events are isolated and examples are given in Figure 1. It shows cases with different frequency patterns: no structure (top panel), time striations (middle panel), and filamentary structures (bottom panel). The latter case is rather rare.

### 3. Properties of the Events

The time length of the 2,526 events is between 1 and 4 min. Their locations are shown in Figure 2 where we clearly see the usual limits of geomagnetic latitudes between  $-65^\circ$  and  $+65^\circ$  for our observations. Oppositely the records in relation with HAARP and EISCAT are at much higher latitudes. We also notice a lack of events at longitudes between  $-80^\circ$  and  $20^\circ$ E. This

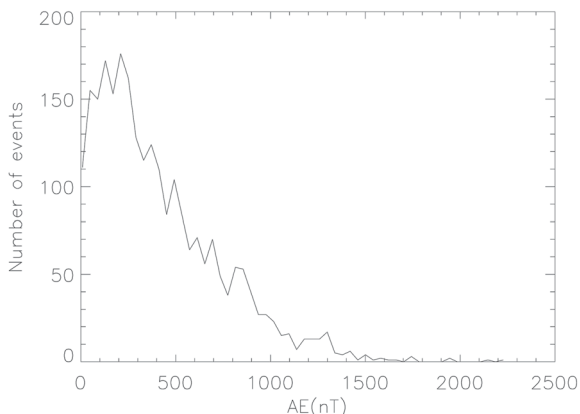


**Figure 5.** Number of events as a function of the substorm AE index.

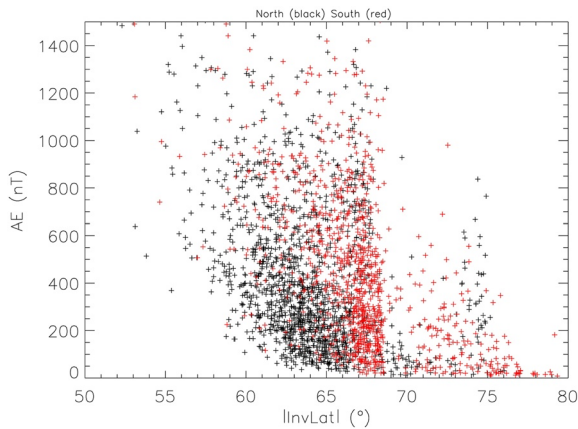


**Figure 6.** Variation of the invariant latitude of the events as a function of the AE index in the Northern hemisphere (black sign +) and in the Southern hemisphere (red sign +).

the auroral oval increases when the magnetic activity decreases (Meng, 1984). This is also observed with our data in Figure 6 which shows that the invariant latitude of our events increases when the substorm AE index decreases. This effect is, however, also linked to the exceptional HAARP and EISCAT operations at high latitudes, which were planned randomly in time with respect to the AE index, and thus statistically more often during low magnetic activity. One can also notice in Figure 6 a slight asymmetry in the locations of the events between the Northern and the Southern hemisphere.

To summarize, the locations of the events are observed independently of the geographic longitude all over the auroral oval both in the North and the South but much more events are observed in the North.

It was shown in Figure 5 that the events do not necessarily occur when the AE index is high as it is for the real AKR (Morioka et al., 2005). A superposed epoch method has been done in Figure 7 to average the AE index as a function of the days around the events. It is shown that the maximum average value of AE is of the order of 430 nT and that it occurs on the same day as the AKR-like events. Of course, when an auroral activity is present, many AKR-like events are recorded during a long time. For example, Figure 8 presents a remarkable sequence of 50 events recorded in the North (panel [a]) and in the South (panel [b]) between 4 April 2010 at 06:01 UT and 7 April 2010 at 21:23 UT during a substorm (see the AE index variation in panel [c]). In the North, four orbits are plotted (three of them

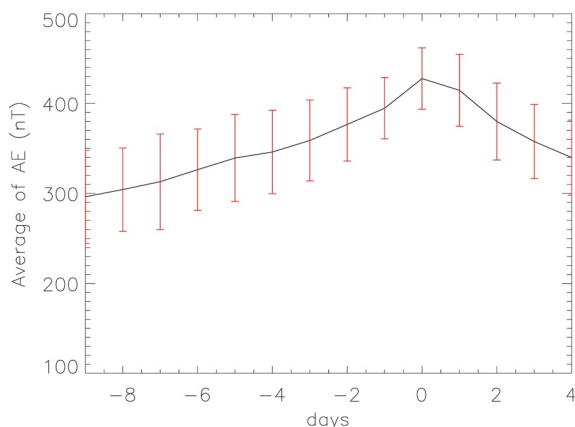


**Figure 7.** Average value of the AE index as a function of the days before and after the 2,526 events. The standard deviations are indicated by red bars.

is emphasized in Figure 3 which shows the number of events as a function of the geographic longitude in the North and in the South.

In fact, this dramatic decrease of events is an artifact due to the operational constraints of the DEMETER data acquisition, which is usually done between  $-65^\circ$  and  $+65^\circ$  of geomagnetic latitude. As the Earth's magnetic field is not symmetric, this operational limit defined in centered dipole coordinates also projects asymmetrically onto coordinates linked to a more realistic model of the magnetic field. For this purpose, we use the invariant latitude, obtained using the IGRF (International Geomagnetic Reference Field) model of the internal field and the Tsyganenko 89 model of the external contributions to the magnetic field. In the polar plots of Figure 4 we clearly see that at longitudes between  $-80^\circ$  and  $20^\circ\text{E}$  the number of recorded events is much lower because the DEMETER measurement limits move to higher invariant latitudes and cut off most of the AKR-like event which might have been otherwise observed there. This explains why there is a lack of events between  $-80^\circ$  and  $20^\circ\text{E}$ .

Figure 5 shows that while some DEMETER events are observed during high substorm activity, the majority of events are recorded during low magnetic activity. On the other hand, it is known that the latitudinal position of the

auroral oval increases when the magnetic activity decreases (Meng, 1984). This is also observed with our data in Figure 6 which shows that the invariant latitude of our events increases when the substorm AE index decreases. This effect is, however, also linked to the exceptional HAARP and EISCAT operations at high latitudes, which were planned randomly in time with respect to the AE index, and thus statistically more often during low magnetic activity. One can also notice in Figure 6 a slight asymmetry in the locations of the events between the Northern and the Southern hemisphere.

are consecutive) where events are seen each time the satellite is over the auroral oval. This gives an idea about the duration of the emissions because it takes approximately 12 min to cross the pole and there is a time gap of 1 hr 40 min between two consecutive orbits. It also shows that the large majority of events occurs during nighttime, and few events are during daytime. This is confirmed with Figure 9 which represents the number of events as a function of MLT in the Northern (green line) and the Southern (red line) hemisphere. Taking into account that DEMETER is nearly sun-synchronous, all MLT values cannot be covered, but one can see that much more events are recorded on the night side than on the day side. One can also see a shift in MLT between the two hemispheres. In the North the maximum is at 20:00 MLT whereas it is at midnight in the South. A similar MLT shift with real AKR has been obtained by Mutel et al. (2004) using the WBD data of the CLUSTER satellites (see their Figure 7). It must be noticed that this shift is also observed with auroras. During a magnetic storm, Østgaard et al. (2018) reported a shift of the order of 3–4 hr in MLT in the aurora imaging between the two hemispheres. Uchida et al. (2020) performed simultaneous observations of auroras at Tjörnnes, Iceland, and Syowa station, Antarctica and they observed a shift of 1.7–2.3 hr in MLT in the South in relation to the North.

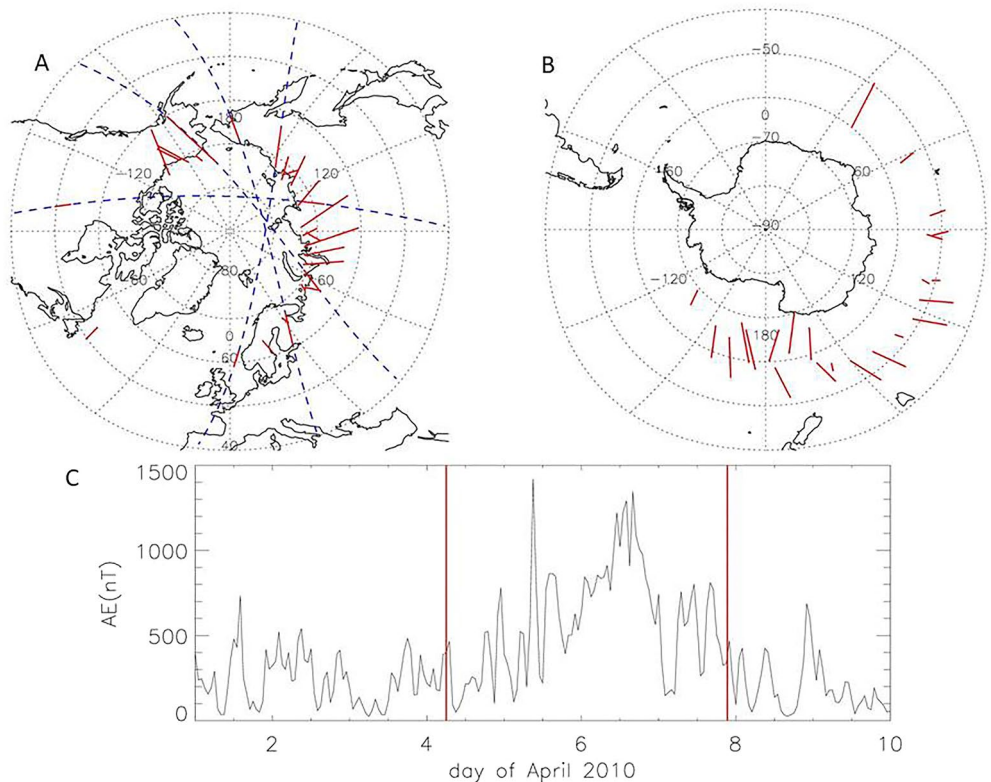


**Figure 8.** Sequence of 50 events (red segments) observed in the North (a) and in the South (b) between 4 April 2010 at 06:01 UT and 7 April 2010 at 21:23 UT at the time of a substorm indicated by the variation of the hourly AE index in panel (c) where the vertical red lines indicate the beginning and the end of this sequence of events. In the panel (a) the dashed blue lines indicate orbits where events are observed on each side of the auroral oval. The power spectrogram of one event is shown in the bottom panel of Figure 1.

The number of events as a function of the invariant latitude is presented in Figure 10 for the Northern (green) and the Southern hemisphere (red). The two curves are very similar and peak around 65° of invariant latitude. A small difference between the North and the South is just observed for the two bumps at higher invariant latitudes (>70°) which correspond to HAARP and EISCAT events. All these characteristics are similar to previous studies of AKR. With 5 years of data from Hawkeye I and Imp 6 satellites, Gallagher and Gurnett (1979) found that the AKR source location is around 65° of invariant latitude and at 22–24 hr in MLT. With the Interball-2 satellite, Schreiber et al. (2002) have shown that the AKR sources were located near 22 hr MLT and 70° of invariant latitude.

These AKR-like events are not very rare. They have been observed during more than 2% of the DEMETER passes above the auroral zones (2,526 over 115,522). One must consider that this is a lowest value of this percentage due to the limit in latitude and the fact that DEMETER was operated during the declining phase of the unusual solar cycle 23 which had an extended minimum (Zerbo et al., 2013). An important point is that there is an asymmetry between the North and the South. The number of events in the North (1,437) is 32% larger than the number of events in the South (1,089) although we have exactly the same number of passes in these two regions. Their occurrence as a function of the months is shown in Figure 11 for the Northern (green) and the Southern hemisphere (red). For each month the number of events is normalized by the corresponding number of half-orbits in this month. It can be seen that this number of events decreases in winter hemispheres with a minimum in December for the North and in June for the South.

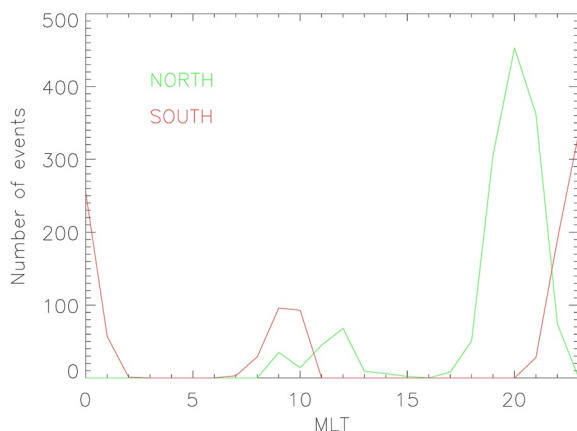


**Figure 9.** Number of events as a function of magnetic local time in the Northern hemisphere (green) and in the Southern hemisphere (red).

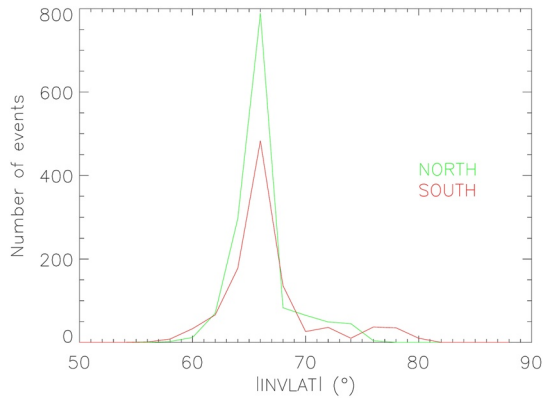


**Figure 10.** Variation of the number of events as a function of the invariant latitude in the North hemisphere (green) and in the South hemisphere (red).

The power spectrum intensity of the events is between  $0.03$  and  $25.0 \mu\text{V}^2 \cdot \text{m}^{-2} \cdot \text{Hz}^{-1}$ . For the subset of the 252 isolated events of AKR-like emissions the frequencies at the maximum intensity have been determined. A histogram of these frequencies is shown in Figure 12. They are mainly between 150 and 600 kHz which corresponds to usual frequencies of the AKR. Under the assumption that AKR-like emissions are due to AKR at higher altitudes, one can consider that the AKR-like frequencies correspond to the frequencies of AKR. It is known that, in the source, AKR is generated at a frequency close to the local electron gyrofrequency and then it is possible from our frequency values of the AKR-like emissions to determine the altitude of the source of the parent AKR using a magnetic field model. This has been done for the 252 events and Figure 13 gives this altitude as a function of the AKR-like frequencies. The altitudes are between 2,000 and 12,000 km which well correspond to usual values for AKR sources. Figure 13 also shows that there is no preference for frequencies/source altitudes in the South and in the North.

Filamentary structures of AKR-like emissions have been rarely observed by DEMETER and an example is shown in the bottom panel of Figure 1. With the South Pole receivers, LaBelle et al. (2022) have also registered such emissions on the ground simultaneously with CLUSTER WBD striated AKR at distances larger than  $10 R_E$ . They noticed that these emissions are rather rare. It was also a comment given by Mutel et al. (2006) and Menietti et al. (2006) who extensively studied the striated AKR with the same WBD experiment onboard CLUSTER. They have detected these striated AKR in less than 1% of all spectra.

#### 4. Discussions and Conclusions

AKR-like emissions observed by DEMETER at low altitudes present many similarities with usual AKR observed at much higher altitudes. But a significant feature is the strong dissymmetry between the Northern and the Southern hemisphere. There are more events in the North than in the South but the difference tends to decrease when the auroral activity increases as it can be seen in Figure 14. Although it is difficult to find the counterpart in the existing literature, a comparison with simultaneous satellite observations of AKR in the two hemispheres was done. With the GEOTAIL data recorded at more than  $10 R_E$ , Kasaba et al. (1997) have shown that the AKR occurrence was asymmetric in the summer and winter hemispheres. They concluded that AKR is more active in the winter hemisphere. Other studies with 7 years of EXOS-D data (Kumamoto & Oya, 1998; Kumamoto et al., 2003) have shown seasonal variations of AKR intensity and occurrence frequency both in the northern and southern hemispheres. They also concluded that AKR emissions are more intense and more numerous in the winter polar regions. These two studies are in complete contradiction with the DEMETER observations about the AKR-like emissions: there is an important decrease during the winter as it is shown in Figure 11. It occurs at the solstice, December in the Northern hemisphere and June in the Southern hemisphere.

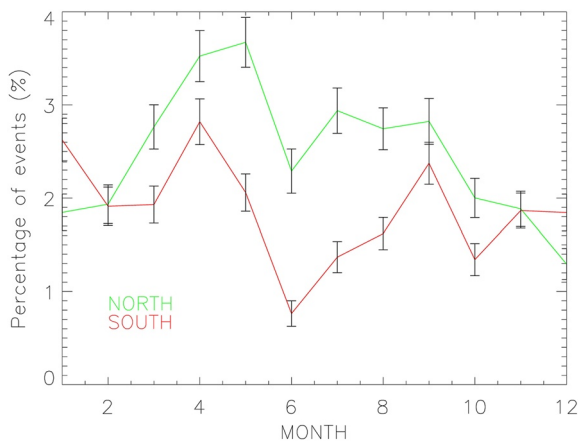


**Figure 11.** Percentage of events per month normalized by the number of registered half-orbits during the corresponding month for the Northern hemisphere (green) and the Southern hemisphere (red). The standard deviations are indicated by black bars.

While there are few studies about simultaneous AKR observations in the two hemispheres, it is different for the observations of auroras. There are numerous reports about auroral asymmetry detected either from ground-based receivers or from satellites (see for example, Liou & Mitchell, 2019; Liou et al., 2018; Luan et al., 2010, 2016; Newell et al., 2010; Østgaard et al., 2015, 2018; Reistad et al., 2013; Uchida et al., 2020). But here also it is difficult to find similar characteristics for the occurrences of AKR-like emissions and auroras. A near fit is provided by the study of Luan et al. (2010) who have calculated in both hemispheres an averaged auroral Hemispheric Power (HP) using the Far-ultraviolet emission recorded by the global ultraviolet imager (GUVI) instrument on board the Thermosphere Ionosphere Mesosphere Energetics and Dynamics (TIMED) satellite during 2002–2007. Under geomagnetically quiet conditions, they claimed that the HP was larger in the summer season/

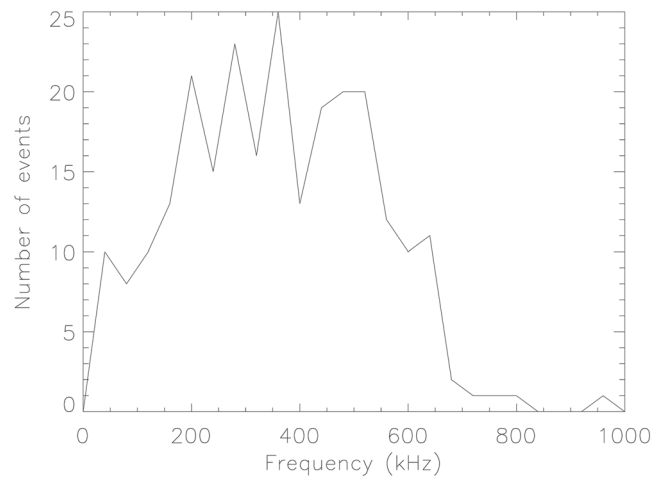


**Figure 12.** Histogram of the frequencies where the intensity of the auroral kilometric radiation-like emissions is maximum. This plot is obtained with the subset of 252 events.

hemisphere than in the winter season/hemisphere. This well fits with the data shown in Figure 11: the AKR-like event percentage of June in the North and December in the South (summer) is larger than the percentage of June in the South and December in the North (winter). They also said that the HP is larger in the southern summer than in the northern summer. But this is less evident with the AKR-like emissions.

Very recently, Pakhotin et al. (2021) used SWARM satellites to show that electromagnetic energy input at 450 km altitude is more important in the Northern hemisphere, and Cosgrove et al. (2022) used FAST satellite to show that the integrated Poynting flux is also larger for the Northern hemisphere than for the Southern hemisphere. Both claimed that it must be due to the offset of the magnetic dipole which is away from the Earth's center. The state-of-the-art mechanisms to explain the auroral asymmetries in conjugate hemispheres is discussed by Østgaard et al. (2015). These mechanisms involve the variations of the interplanetary magnetic field, the field-aligned currents, and the ionospheric conductivity.

To understand such discrepancy between the AKR-like emissions and the AKR, one can say that, to observe the DEMETER events, favorable conditions for the AKR generation are of course needed, but also favorable conditions for the leaked AKR generation and favorable conditions for the propagation of the leaked AKR down in the dense ionosphere must be present. The combination of these three processes can lead to differences between the occurrence of AKR and the occurrence of AKR-like emissions at low altitudes.

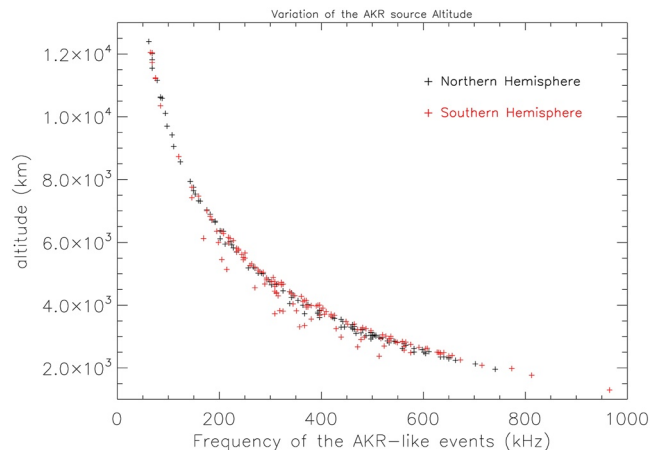


**Figure 13.** Variation of the source altitude of the expected parent auroral kilometric radiation (AKR) as a function of the frequency of the AKR-like events for the North (black +) and the South (red +). See text for explanation.

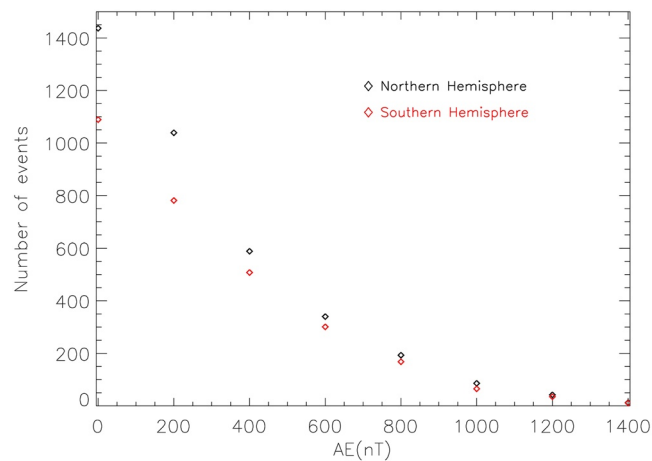


**Figure 14.** Number of events in the North (black diamond) and in the South (red diamond) when AE is larger than the value indicated on the horizontal axis.

Despite an important constraint concerning the lack of observations at very high latitudes, the data set of AKR-like emissions recorded by DEMETER both in the Northern and Southern auroral zones during 6.5 years is a unique opportunity to determine the characteristics of these emissions. The main conclusions are as follows:

1. These events are not very rare: on average, they are observed in about 2% of auroral zone crossings and even it can reach 3.7% in May in the Northern hemisphere (see Figure 11),
2. They have characteristics similar to the AKR at higher altitudes: occurrence in the same frequency range (150–600 kHz), in the same MLT sector (20–0), at the same invariant latitude (65°),
3. They occur mainly during moderate auroral activity (AE of the order of 430 nT),
4. There is a shift in MLT for the events in the South in relation to the North.
5. There is a strong asymmetry between the North and the South: more events are observed in the Northern hemisphere than in the Southern hemisphere (on average by 32%). This difference decreases when AE increases.
6. There is a seasonal effect which is similar in each hemisphere: the number of events decreases in winter hemispheres.

Concerning the two last points, one cannot find similar behaviors in the observations either of AKR at higher altitudes with satellites or of auroras with optical photometers on ground or onboard satellites.

## Conflict of Interest

The authors declare no conflicts of interest relevant to this study.

## Data Availability Statement

The DEMETER data shown in this paper can be obtained at <https://cdpp-archive.cnes.fr/>. The AE values are from the WDC for geomagnetism in Kyoto. The values of the Earth's magnetic field have been extracted on line from [https://ccmc.gsfc.nasa.gov/modelweb/models/igrf\\_vitmo.php](https://ccmc.gsfc.nasa.gov/modelweb/models/igrf_vitmo.php); <https://www.agu.org/Publish-with-AGU/Publish/Author-Resources/Grammar-Style-Guide#referenceformat>.

## Acknowledgments

The satellite DEMETER was operated by the French Center National d'Etudes Spatiales (CNES). This work is based on the observations with the electric field experiment ICE embarked on DEMETER. The author thanks J. J. Berthelier the PI of this experiment for the use of the data. F.N. acknowledges the support of the GACR Grant 21-01813S.

## References

- Alexander, J. K., & Kaiser, M. L. (1976). Terrestrial kilometric radiation, 1. Spatial structure studies. *Journal of Geophysical Research*, *81*(34), 5948–5956. <https://doi.org/10.1029/ja081i034p05948>
- Benediktov, E. A., Getmantsev, G. G., Mitjakov, N. A., Rapoport, V. O., Sazonov, J. A., & Tarasov, A. F. (1966). Intensity measurements of radiation at frequencies 725 and 1525 kc by means of the receiver on the satellite Elektron-2. *Advances in Space Research*, *4*, 110.
- Benediktov, E. A., Getmantsev, G. G., Sazonov, Y. A., & Tarasov, A. F. (1965). Preliminary results of measurements of the intensity of distributed extraterrestrial radio-frequency emission at 725 and 1525-kHz frequencies by the satellite Elektron-2. *Cosmic Research*, *3*, 492. (English translation of *Kosmicheskie Issledovaniya* 3, 614–617).

- Benson, R. F., Desch, M. D., Hunsucker, R. D., & Romick, G. J. (1988). Ground-level detection of low-and medium-frequency auroral radio emissions. *Journal of Geophysical Research*, 93(A1), 277–283. <https://doi.org/10.1029/ja093ia01p00277>
- Benson, R. F., & Wong, H. K. (1987). Low-altitude ISIS 1 observations of auroral radio emissions and their significance to the cyclotron maser instability. *Journal of Geophysical Research*, 92(A2), 1218–1230. <https://doi.org/10.1029/JA092iA02p01218>
- Berthelier, J. J., Godefroy, M., Leblanc, F., Malingre, M., Menvielle, M., Lagoutte, D., et al. (2006). ICE, the electric field experiment on DEMETER. *Planetary and Space Science*, 54(5), 456–471. <https://doi.org/10.1016/j.pss.2005.10.016>
- Carpenter, D. L., Bell, T. F., Inan, U. S., Benson, R. F., Sonwalkar, V. S., Reinisch, B. W., & Gallagher, D. L. (2003). Z-mode sounding within propagation “cavities” and other inner magnetospheric regions by the RPI instrument on the IMAGE satellite. *Journal of Geophysical Research*, 108(A12), 1421. <https://doi.org/10.1029/2003JA010025>
- Cosgrove, R. B., Bahcivan, H., Chen, S., Sanchez, E., & Knipp, D. (2022). Violation of hemispheric symmetry in integrated Poynting flux via an empirical model. *Geophysical Research Letters*, 49(4), e2021GL097329. <https://doi.org/10.1029/2021GL097329>
- Gallagher, D. L., & Gurnett, D. A. (1979). Auroral kilometric radiation: Time averaged source location. *Journal of Geophysical Research*, 84(A11), 6501–6509. <https://doi.org/10.1029/ja084ia11p06501>
- Gurnett, D. A. (1974). The Earth as a radio source – Terrestrial kilometric radiation. *Journal of Geophysical Research*, 79(28), 4227–4238. <https://doi.org/10.1029/JA079i028p04227>
- Kasaba, Y., Matsumoto, H., Hashimoto, K., & Anderson, R. R. (1997). The angular distribution of auroral kilometric radiation observed by the GEOTAIL spacecraft. *Geophysical Research Letters*, 24(20), 2483–2486. <https://doi.org/10.1029/97gl02599>
- Krasovskiy, V. L., Kushnerevskiy, Y. V., Mugulin, V. V., Orayevskiy, V. N., & Pulinets, S. A. (1983). Ballistic wave transformation as a mechanism for the linkage of terrestrial kilometric radio waves with low frequency noise in the upper atmosphere. *Geomagnetism and Aeronomy*, 23(6), 702.
- Kumamoto, A., Ono, T., Iizima, M., & Oya, H. (2003). Seasonal and solar cycle variations of the vertical distribution of the occurrence probability of auroral kilometric radiation sources and of upflowing ion events. *Journal of Geophysical Research*, 108(A1), 1032. <https://doi.org/10.1029/2002JA009522>
- Kumamoto, A., & Oya, H. (1998). Asymmetry of occurrence-frequency and intensity of AKR between summer polar region and winter polar regions sources. *Geophysical Research Letters*, 25(13), 2369–2372. <https://doi.org/10.1029/98gl01715>
- Kurth, W. S., Baumbach, M. M., & Gurnett, D. A. (1975). Direction-finding measurements of auroral kilometric radiation. *Journal of Geophysical Research*, 80(19), 2764–2770. <https://doi.org/10.1029/ja080i019p02764>
- LaBelle, J., & Anderson, R. R. (2011). Ground-level detection of auroral kilometric radiation. *Geophysical Research Letters*, 38(4), L04104. <https://doi.org/10.1029/2010GL046411>
- LaBelle, J., Yan, X., Broughton, M., Pasternak, S., Dombrowski, M., Anderson, R. R., et al. (2015). Further evidence for a connection between auroral kilometric radiation and ground-level signals measured in Antarctica. *Journal of Geophysical Research: Space Physics*, 120(3), 2061–2075. <https://doi.org/10.1002/2014JA020977>
- LaBelle, J., Yearby, K., & Pickett, J. S. (2022). South Pole Station ground-based and Cluster satellite measurements of leaked and escaping Auroral Kilometric Radiation. *Journal of Geophysical Research: Space Physics*, 127(2), e2021JA029399. <https://doi.org/10.1029/2021JA029399>
- Liou, K., & Mitchell, E. J. (2019). Hemispheric asymmetry of the pre-midnight aurora associated with the dawn-dusk component of the interplanetary magnetic field. *Journal of Geophysical Research: Space Physics*, 124(3), 1625–1634. <https://doi.org/10.1029/2018JA025953>
- Liou, K., Sotirelis, T., & Mitchell, E. J. (2018). North-south asymmetry in the geographic location of auroral substorms correlated with ionospheric effects. *Scientific Reports*, 8(1), 1–6. <https://doi.org/10.1038/s41598-018-35091-2>
- Louarn, P. (2006). Generation of auroral kilometric radiation in bounded source regions. In *Geospace electromagnetic waves and radiation* (pp. 55–86). Springer.
- Luan, X., Wang, W., Burns, A., & Dou, X. (2016). Universal time variations of the auroral hemispheric power and their interhemispheric asymmetry from TIMED/GUVI observations. *Journal of Geophysical Research: Space Physics*, 121(10), 10258–10268. <https://doi.org/10.1002/2016JA022730>
- Luan, X., Wang, W., Burns, A., Solomon, S., Zhang, Y., & Paxton, L. J. (2010). Seasonal and hemispheric variations of the total auroral precipitation energy flux from TIMED/GUVI. *Journal of Geophysical Research*, 115(A11), A11304. <https://doi.org/10.1029/2009JA015063>
- Meng, C. I. (1984). Dynamic variation of the auroral oval during intense magnetic storms. *Journal of Geophysical Research*, 89(A1), 227–235. <https://doi.org/10.1029/ja089ia01p00227>
- Menietti, J. D., Mutel, R. L., Santolík, O., Scudder, J. D., Christopher, I. W., & Cook, J. M. (2006). Striated drifting auroral kilometric radiation bursts: Possible stimulation by upward traveling EMIC waves. *Journal of Geophysical Research*, 111(A4), A04214. <https://doi.org/10.1029/2005JA011339>
- Morioka, A., Miyoshi, Y. S., Tsuchiya, F., Misawa, H., Kumamoto, A., Oya, H., et al. (2005). Auroral kilometric radiation activity during magnetically quiet periods. *Journal of Geophysical Research*, 110(A11), A11223. <https://doi.org/10.1029/2005JA011204>
- Mutel, R. L., Christopher, I. W., Menietti, J. D., Gurnett, D. A., Pickett, J. S., Masson, A., et al. (2011). RX and Z-mode growth rates and propagation at cavity boundaries. In H. O. Rucker, W. S. Kurth, P. Louarn, & G. Fischer (Eds.), *Planetary radio emissions VII* (pp. 241–252). Austrian Academy of Sciences.
- Mutel, R. L., Gurnett, D. A., & Christopher, I. W. (2004). Spatial and temporal properties of AKR burst emission derived from Cluster WBD VLBI studies. *Annales Geophysicae*, 22(7), 2625–2632. <https://doi.org/10.5194/angeo-22-2625-2004>
- Mutel, R. L., Menietti, J. D., Christopher, I. W., Gurnett, D. A., & Cook, J. M. (2006). Striated auroral kilometric radiation emission: A remote tracer of ion solitary structures. *Journal of Geophysical Research*, 111(A10), A10203. <https://doi.org/10.1029/2006JA011660>
- Newell, P. T., Sotirelis, T., & Wing, S. (2010). Seasonal variations in diffuse, monoenergetic, and broadband aurora. *Journal of Geophysical Research*, 115(A3), A03216. <https://doi.org/10.1029/2009JA014805>
- Østgaard, N., Reistad, J. P., Tenfjord, P., Laundal, K. M., Rexer, T., Haaland, S. E., et al. (2018). The asymmetric geospace as displayed during the geomagnetic storm on 17 August 2001. *Annales Geophysicae*, 36(6), 1577–1596. <https://doi.org/10.5194/angeo-36-1577-2018>
- Østgaard, N., Reistad, J. P., Tenfjord, P., Laundal, K. M., Snekvik, K., Milan, S., & Haaland, S. (2015). Mechanisms that produce auroral asymmetries in conjugate hemispheres. *Auroral dynamics and space weather*, 215, 133–143.
- Oya, H., Morioka, A., & Obara, T. (1985). Leaked AKR and terrestrial hectometric radiations discovered by the plasma wave and sounder experiments on the EXOS-C satellite—Instrumentation and observation results of plasma wave phenomena. *Journal of Geomagnetism and Geoelectricity*, 37(3), 237–262. <https://doi.org/10.5636/jgg.37.237>
- Pakhotin, I. P., Mann, I. R., Xie, K., & Knudsen, D. J. (2021). Northern preference for terrestrial electromagnetic energy input from space weather. *Nature Communications*, 12(1), 199. <https://doi.org/10.1038/s41467-020-20450-3>
- Parrot, M., & Berthelier, J.-J. (2012). AKR-like emissions observed at low altitude by the DEMETER satellite. *Journal of Geophysical Research*, 117(A10), A10314. <https://doi.org/10.1029/2012JA017937>

- Reistad, J. P., Østgaard, N., Laundal, K. M., & Oksavik, K. (2013). On the non-conjugacy of nightside aurora and their generator mechanisms. *Journal of Geophysical Research*, *118*(6), 3394–3406. <https://doi.org/10.1002/jgra.50300>
- Schreiber, R., Santolik, O., Parrot, M., Lefeuvre, F., Hanasz, J., Brittnacher, M., & Parks, G. (2002). Auroral kilometric radiation source characteristics using ray tracing techniques. *Journal of Geophysical Research*, *107*(A11), SMP 20-1–SMP 20-7. <https://doi.org/10.1029/2001JA009061>
- Treumann, R. A., Baumjohann, W., & LaBelle, J. (2018). Sub-ionospheric AKR: A possible mechanism for its transport down from the topside generation region to the F layer and ground. arXiv preprint arXiv:1803.10956.
- Uchida, H. A., Kataoka, R., Kadokura, A., Murase, K., Yukimatu, A. S., Miyoshi, Y., et al. (2020). Asymmetric development of auroral surges in the Northern and Southern Hemispheres. *Geophysical Research Letters*, *47*(13), e2020GL088750. <https://doi.org/10.1029/2020GL088750>
- Wu, C. S., & Lee, L. C. (1979). A theory of the terrestrial kilometric radiation. *The Astrophysical Journal*, *230*, 621–626. <https://doi.org/10.1086/157120>
- Zerbo, J. L., Amory-Mazaudier, C., & Ouattara, F. (2013). Geomagnetism during solar cycle 23: Characteristics. *Journal of Advanced Research*, *4*(3), 265–274. <https://doi.org/10.1016/j.jare.2012.08.010>